JOURNAL OF AGRICULTURAL AND FOOD CHEMISTRY
ARTICLE

J. Agric. Food Chem. 2009, 57, 4403–4408 4403
DOI:10.1021/jf900045p

Cloning, Expression, and Purification of a Functional Glutathione Reductase from Sweet Potato (*Ipomoea batatas* [L.] Lam): Kinetic Studies and Characterization

Cheng-Jen Chen,[†,∥] Chih-Yu Huang,[†,∥] Jenq-Kuen Huang,[‡,∥] Choa-Yi Lin,[§,∥] and Chi-Tsai Lin*,[†]

[†]Institute of Bioscience and Biotechnology and Center for Marine Bioscience and Biotechnology, National Taiwan Ocean University, Keelung 202, Taiwan, [‡]Department of Chemistry, Western Illinois University, 1 University Circle, Macomb, Illinois 61455-1390, and [§]Graduate Institute of Medical Sciences, Taipei Medical University 110, Taiwan. [∥] These authors contributed equally to this work.

A cDNA encoding a putative glutathione reductase (GR) was cloned from sweet potato (Ib). The deduced protein showed high level of sequence homology with GRs from other plants (79−38%). A three-dimensional (3-D) homology structure was created. The active site Cys residues are conserved in all reported GR. Functional IbGR was overexpressed and purified. The purified enzyme showed an active monomeric form on a 10% native polyacrylamide gel electrophoresis (PAGE). The monomeric nature of the enzyme was confirmed by sodium dodecyl sulfate−polyacrylamide gel electrophoresis (SDS−PAGE) and molecular mass determination of the native enzyme. The Michaelis constant (K_m) values for GSSG (glutathione disulfide) and NADPH (β-nicotinamide adenine dinucleotide phosphate, reduced form) were 0.114 and 0.056 mM, respectively. The enzyme activity was inhibited by Cu^{2+} and Zn^{2+}, but not by Ca^{2+}. The protein's half-life of deactivation at 70 °C was 3.3 min, and its thermal inactivation rate constant K_d was 3.48×10^{-1} min^{-1}. The enzyme was active in a broad pH range from 6.0 to 11.0 and in the presence of imidazole up to 0.8 M. The native enzyme appeared to be resistant to digestion by trypsin or chymotrypsin.

KEYWORDS: Sweet potato (*Ipomoea batatas* [L.] Lam); three-dimensional homology structure (3-D homology structure); expression; glutathione reductase (GR)

INTRODUCTION

Sweet potato is widely distributed in Taiwan. It is considered as one of the cash crops sustaining the agricultural economy. This local crop is highly regarded in Taiwan. Several components from sweet potato have been shown to exhibit antioxidative effects (*1*−*7*). Although sweet potato shows physiological activities with potential medical applications (*8*), only several scientific studies have been reported. This encourages us to search active components from the root of sweet potato for use.

Plants have multiple defense mechanisms involving small molecular antioxidants and enzymes, which prevent the formation or scavenge ROS (reactive oxygen species). Small molecular antioxidants such as glutathione, ascorbate, and tocopherol control the levels of ROS in plant tissues (*9*). A major component of these defense mechanisms is the ascorbate−glutathione cycle involving four enzymes: glutathione reductase (GR), ascorbate peroxidase, dehydroascorbate reductase, and monodehydroascorbate reductase (*10*). GR (EC 1.6.4.2) participates in the removal of H_2O_2 via recycling of the GSH (reduced form of glutathione) pool, thus playing a central role during oxidative stress (*11*). Most of the ascorbate−glutathione cycle enzymatic activities, including GR, are located in chloroplasts, cytosol, mitochondria, and peroxisomes (*12*). However, only two forms of GR genes have been identified to date, a cytosolic isoform (cGR) and an isoform dual targeted (dtGR) to both chloroplasts and mitochondria (*13*, *14*).

Here, we report cloning of a putative IbGR cDNA from sweet potato. The coding region of the cDNA was introduced into a yeast expression system. The target protein was overexpressed and showed high levels of activity in catalyzing GSSG to GSH. The recombinant enzyme has been purified and its properties investigated.

MATERIALS AND METHODS

Sweet Potato (*Ipomoea batatas* [L.] Lam). Sweet potato was grown in a field located at the north part of Taiwan (kindly provided by Professor Rong-Huay Juang, Department of Biochemical Science and Technology, National Taiwan University, Taiwan).

*To whom correspondence should be addressed. Institute of Bioscience and Biotechnology, National Taiwan Ocean University, 2 Pei-Ning Rd, Keelung 202, Taiwan. Phone: 886-2-24622192 ext. 5513. Fax: 886-2-24622320. E-mail: B0220@mail.ntou.edu.tw.

© 2009 American Chemical Society Published on Web 4/9/2009

Total RNA Preparation and cDNA Synthesis. The tuberous root of the sweet potato (wet weight 3 g) was frozen in liquid nitrogen and ground to powder in a ceramic mortar. PolyA mRNA (24 μg) was prepared using Straight A's mRNA Isolation System (Novagen). Six micrograms of the mRNA was used in 5′-RACE-Ready cDNA and 3′-RACE-Ready cDNA synthesis using Clontech's SMART RACE cDNA Amplification Kits.

Isolation of GR cDNA. Using the 5′-RACE-Ready cDNA of sweet potato as a template and UPM primer (universal primer A mix, purchased from BD biosciences) and a degenerate primer (5′ CAT CWC CHA CAG CCC ATA T 3′), a 1,079 bp fragment was amplified by PCR. The degenerate primer was designed on the basis of the conserved sequences of GR from BrGR (*Brassica rapa*, AAF67753) and PsGR (*Pisum sativum*, CAA66924). The 1,079 bp fragment was subcloned and sequenced. On the basis of this DNA sequence, a forward primer (5′ GCA ACA GGC AGT AGG GCT CAG 3′) near the 3′-end of the 1,079 bp fragment was synthesized. The forward primer allowed sequence extension to the 3′-end of the 1,079 bp fragment. Using the 3′-RACE-Ready cDNA of sweet potato as a template, a 1,479 bp fragment was amplified by PCR. This DNA fragment was subcloned and sequenced. Sequence analysis revealed that the combined sequence of the 1,079 bp and the 1,479 bp covered an open reading frame of IbGR cDNA (2,062 bp, EMBL accession no. EU137675). The identity of the GR cDNA clone was assigned by comparing the DNA sequence and inferring the amino acid sequence in various data banks using the basic local alignment search tool (BLAST).

Computational Analysis. The blast program was used to search homologous protein sequences in the nonredundant database at the National Center for Biotechnology Information, National Institutes of Health (http://www.ncbi.nlm.nih.gov/). Multiple alignments were constructed using the ClustalW2 program (http://www.ebi.ac.uk/Tools/clustalw2/index.html). Structural modeling was carried out by using the SWISS-MODEL program (*15*) (http://swissmodel.expasy.org/SWISS-MODEL.html) to create a 3-D homology model based on the known X-ray structure of GR (PDB code 1GER) from *E. coli* (*16*). The modeling data was then superimposed with the EcGR by DeepView Swiss-PdbViewer v3.7 (http://www.expasy.org/spdbv/) (*15*).

Construction of the Coding GR cDNA in an Expression Vector. The coding region of the GR cDNA was amplified using gene specific flanking primers. The 5′ upstream primer contains the *Eco*RI recognition site (5′ GAATTCG ATG GCA AGG AAG ATG TTA AA 3′), and the 3′ downstream primer contains 6His-tag and *Eco*RI recognition site (5′ GAATTCCTA GTG GTG GTG GTG GTG GTG GTC CTC 3′). Using 0.2 μg of IbGR cDNA as a template, and 10 pmol of each 5′ upstream and 3′ downstream primers, a 1.5 kb fragment was amplified by PCR. The fragment was ligated into pCR4 and transformed into *E. coli*. The recombinant plasmid was isolated and digested with *Eco*RI. The digestion products were separated on a 1% agarose gel. The 1.5 kb DNA insert was gel purified and subcloned into the *Eco*RI site of pYEX-S1 expression vector (Clontech) and introduced into *Saccharomyces cerevisiae* (trp^- ura^-). The transformed yeast cells were selected by YNBD (0.17% yeast nitrogen base, 0.5% ammonium sulfate, and 2% glucose) agar plates containing 20 μg of Trp/mL. The presence of GR cDNA in the selected transformants was verified by PCR using gene specific flanking primers. The recombinant IbGR protein was expressed in yeast in YPD medium (1% yeast extract, 2% peptone, and 2% glucose). Functional recombinant IbGR protein was identified by an activity assay as described below.

Expression and Purification of the Recombinant IbGR. The transformed yeast containing the IbGR was grown at 30 °C in 250 mL of YPD medium for 5 days. The cells were harvested and soluble proteins extracted in PBS with glass beads as described before (*17*). The recombinant IbGR was purified by Ni-NTA affinity chromatography (elution buffer: 1/3 PBS containing 100 mM imidazole) as per the manufacturer's instructions (Qiagen). The purified protein was checked by SDS−PAGE (10% acrylamide) and native PAGE. Proteins on the gel were detected by staining with Coomassie brilliant blue.

Molecular Mass Determination by Q-TOF ESI/MS/MS. The protein sample (135 μg/50 μL) in 0.003× PBS containing 0.05% glycerol was shipped to Yao-Hong Biotechnology Company (Taiwan) for molecular mass determination using Q-TOF ESI/MS/MS mass spectrometry (Micromass, Manchester, England).

Protein Concentration Determination. Protein concentration was determined by a Bio-Rad Protein Assay Kit (Bio-Rad Laboratories) using bovine serum albumin as a standard.

IbGR Activity Assay and Kinetic Studies. IbGR was assayed by measuring GSSG-dependent NADPH oxidation (*18*, *19*) with some modification. The recombinant sweet potato IbGR activities were tested at 25 °C by monitoring the oxidation of NADPH at A_{340} for GSSG reduction. The kinetic properties of the IbGR (0.2 μg) in a total volume of 100 μL assay mixture containing 100 mM potassium phosphate buffer (pH 8.0) was determined using different concentrations of GSSG (0.08 to 0.14 mM) with either the fixed amount of 0.2 mM NADPH as substrate or using different concentrations of NADPH (0.04 to 0.2 mM) with the fixed amount of 0.1 mM GSSG.. The absorbance at 340 nm was recorded between 30 to 60 s for detecting different concentrations of GSSG or between 10 to 30 s for detecting different concentrations of NADPH. The absorbance coefficient of NADPH at 340 nm is $\varepsilon = 6.22 \times 10^3$ M^{-1} cm^{-1}. The K_m, V_{max}, and k_{cat} were calculated from Lineweaver−Burk plots.

Enzyme Characterization. The IbGR activity was tested under various conditions. Aliquots of IbGR were subjected to various treatments as described below and then assayed for activity.

(1) Effect of Divalent Ions on Enzyme Activity. The enzyme activity was carried out as mentioned in IbGR Activity Assay and Kinetic Studies in the presence of various divalent ions. The concentration of IbGR was 0.2 μg/reaction, and the final concentrations of Ca^{2+} ($CaCl_2$), Zn^{2+} ($ZnSO_4$), and Cu^{2+} ($CuSO_4$) were 1, 5, and 10 mM, respectively. Each sample was incubated at 37 °C for an hour.

(2) Effect of Heat on Enzyme Activity. Enzyme samples were preheated at 70 °C for 2, 4, 8, or 16 min, respectively.

(3) Effect of pH on Enzyme Activity. The enzyme sample was adjusted to the desired pH by adding a half volume of buffer with different pH values: 0.2 M citrate buffer (pH 2.5 or 4.0), 0.2 M potassium phosphate buffer (pH 6.0, 7.0, or 8.0), or 0.2 M CAPS buffer (pH 10.0 or 11.0). Each sample was incubated at 37 °C for an hour.

(4) Effect of Imidazole on Enzyme Activity. During protein purification, the GR enzyme was eluted with imidazole. Therefore, the effect of imidazole on protein activity/stability was examined. Imidazole was added to a final concentration of 0.2, 0.4, or 0.8 M and incubated at 37 °C for an hour.

(5) Proteolytic Susceptibility. The enzyme was incubated with one-tenth its weight of trypsin or chymotrypsin at pH 8.0 and 37 °C for 10, 20, or 40 min. In the chymotrypsin digestion, $CaCl_2$ was added to 5 mM. Aliquots were removed at various time intervals for analysis.

RESULTS

Cloning, Sequence Alignment, and Structure Modeling of a cDNA Encoding IbGR. A putative IbGR cDNA clone was identified on the basis of the consensus pattern and sequence homology to the published GRs. The IbGR cDNA (2,062 bp, EMBL accession no. EU137675) contains an open reading frame, which encodes a protein of 494 amino acid residues with a predicted molecular mass of 54 kDa. **Figure 1A** shows the amino acid sequence alignment of the putative sweet potato IbGR with GRs from several sources. The IbGR shared 79, 79, 79, 78, and 38% sequence identity with GR from BrGR (*Brassica rapa*, AAF67753), PsGR (*Pisum sativum*, CAA66924), VuGR (*Vigna unguiculata*, ABB89042), PvGR (*Phaseolus vulgaris,* ABF29524), and EcGR (*Escherichia coli*, P06715). A structural model of IbGR was created on the basis of the known structure of GR from *E. coli* via the SWISS-MODEL program and was superimposed with the SPDBV_4 program to obtain a better structure. Superimposition of IbGR (pink) and *E. coli* GR (gray) was shown by using protein solid ribbons. The two residues coordinating active sites Cys70 and Cys75 are conserved as they are present in all reported GR sequences. The upper blue ball represents the active site (**Figure 1B**).

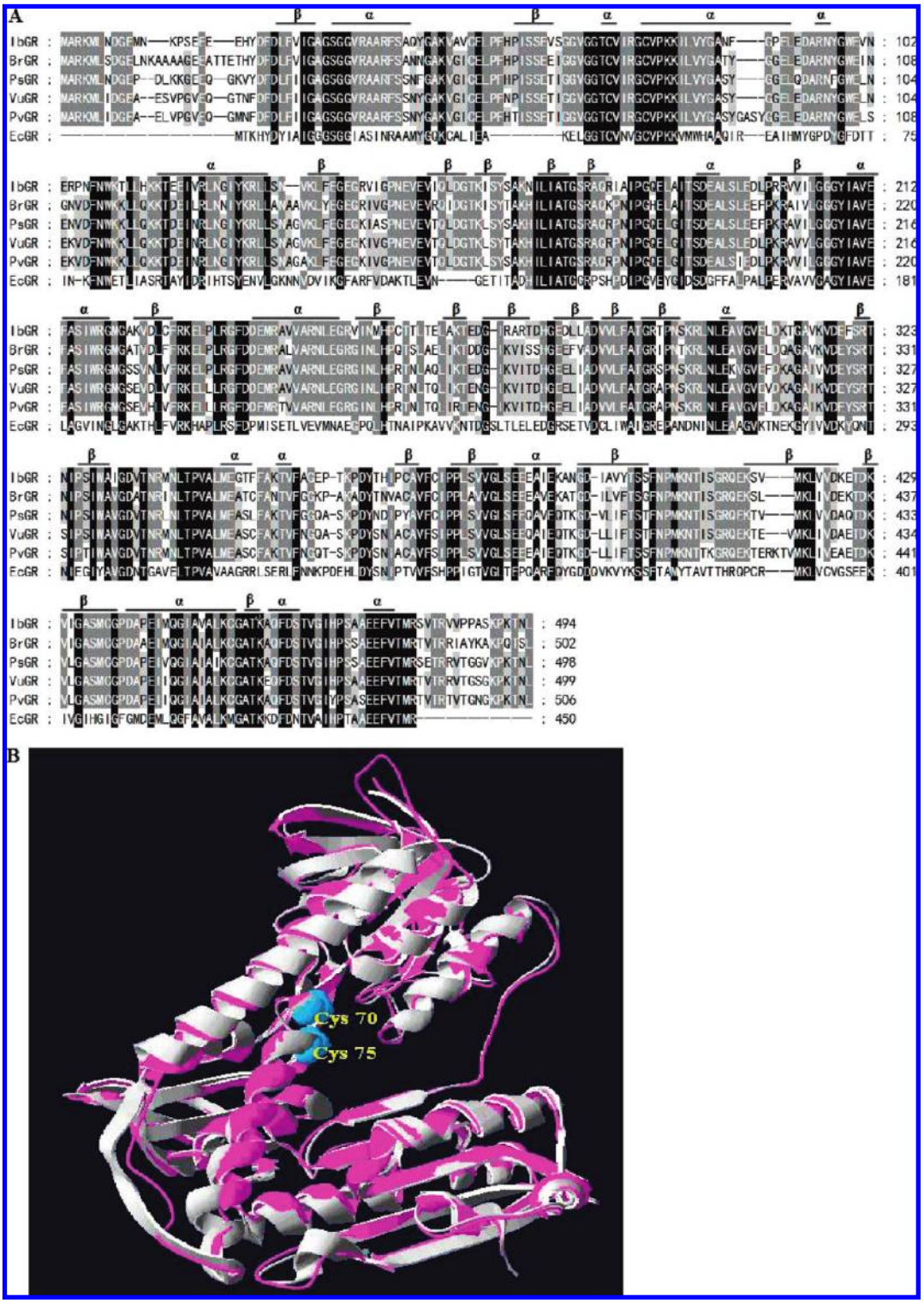

Figure 1. Optimal alignment of the amino acid sequences of GR from various sources and homology structure prediction. (**A**) Sequence alignment: IbGR (present study), BrGR (*Brassica rapa*); PsGR (*Pisum sativum*); VuGR (*Vigna unguiculata*); PvGR (*Phaseolus vulgaris*); and EcGR (*Escherichia coli*). Identical amino acids in all sequences are shaded black, and conservative replacements are shaded gray. The protein secondary structure was predicted by the SWISS-MODEL program and represented as α helices and β strands. (**B**) Three-dimensional homology model of IbGR. The model was created by SWISS-MODEL based on the known X-ray structure of *E. coli* GR. They were superimposed with the SPDBV_4 program. Superimposition of IbGR (pink) and *E. coli* GR (gray) was shown by using the protein solid ribbon. The two residues coordinating active site Cys70 and Cys75 are conserved as they are present in all reported GR sequences. The upper blue ball represents the active site.

Expression and Purification of the Sweet Potato IbGR. The cDNA was introduced into the yeast expression system as described in Materials and Methods. The recombinant IbGR protein was overexpressed and the total cellular proteins analyzed by SDS−PAGE (**Figure 2**). The IbGR fusion protein was purified by Ni-NTA affinity chromatography. The progress of purification was monitored by SDS−PAGE as shown in **Figure 2**. The results showed that the IbGR protein was purified to homogeneity in a single step. Only monomeric GR was detected in these fractions suggesting that sweet potato IbGR

is composed of a monomer with an apparent molecular mass of 54.8 kDa. The mass of IbGR was 54.6 kDa as analyzed using Q-TOF ESI/MS/MS. The result confirms the presence of the monomer under the conditions of 0.003× PBS containing 0.05% glycerol. When using native PAGE to analyze the IbGR, only one protein band was seen in **Figure 5B**. This again indicates that the enzyme is monomeric in nature. The yield of the purified IbGR was 1.350 mg per 250 mL of culture.

Kinetic Studies of the Purified IbGR. As shown in **Figure 3A−B**, the Lineweaver−Burk plot of the velocity ($1/V$) against 1/GSSG gave K_m = 0.114 mM, V_{max} = 0.112 mM/min, and k_{cat} = 3,008.25 min^{-1}. The plot of the velocity ($1/V$) against 1/NADPH gave K_m = 0.056 mM, V_{max} = 0.120 mM/min, and k_{cat} = 3,223.12 min^{-1} for the IbGR.

Characterization of the Purified IbGR. Effect of varying concentrations of Ca^{2+}, Zn^{2+}, or Cu^{2+} on enzyme activities is presented in **Figure 4**. The results showed that Cu^{2+} was most effective in reducing IbGR activities. In the presence of 1 mM of Ca^{2+}, Zn^{2+}, or Cu^{2+}, approximately 95%, 55%, and 5% of the IbGR activity was detected, respectively. Thermal effect of the IbGR was examined as described in Materials and Methods. SDS−PAGE analysis of the heat-treated enzyme samples showed the same intensity bands demonstrating that the same amount of enzyme was used in each treatment (**Figure 5A**). The amount of native enzyme decreased with increasing heating time (**Figure 5B**). The enzyme's inactivation kinetics at 70 °C fitted

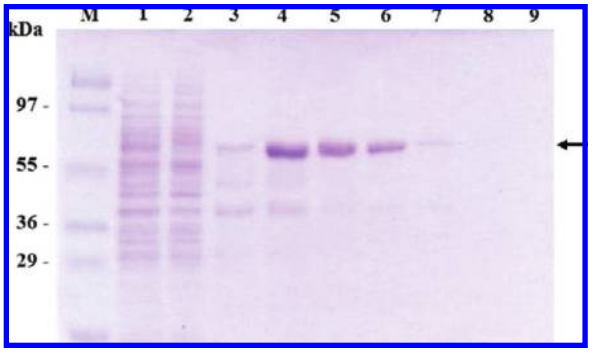

Figure 2. Coomassie-blue-stained SDS−polyacrylamide gel showing the purification of IbGR. Fifteen microliters of each fraction was loaded per lane. Lane 1, crude extract from yeast expressing IbGR; 2, flow-through proteins from the Ni-NTA column; 3, bound GR eluted from Ni-NTA column by 40 mM imidazole; 4, bound GR eluted from the Ni-NTA column by 60 mM imidazole; 5−9, bound GR eluted from the Ni-NTA column by 100 mM imidazole. Molecular masses (in kDa) of standards are shown on the left.

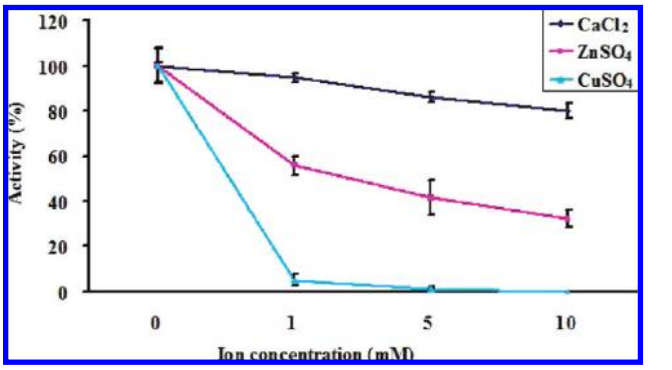

Figure 4. Effect of various concentrations of Ca^{2+}, Zn^{2+}, or Cu^{2+} on enzyme activities. The enzyme sample was adjusted to the desired divalent ion (Ca^{2+}, Zn^{2+}, or Cu^{2+}) concentrations (1, 5, or 10 mM) at 37 °C for 1 h and then assayed for GR activity (0.2 μg protein/reaction). Data are means of three experiments.

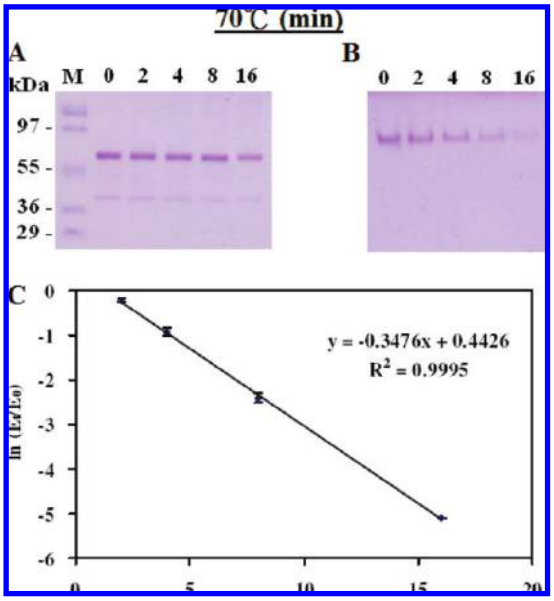

Figure 5. Effect of temperature on purified IbGR. The enzyme sample was heated at 70 °C for various time intervals. Aliquots of the sample were taken at 0, 2, 4, 8, or 16 min then separated by 10% SDS−PAGE and 10% native PAGE. (**A**) 10% SDS−PAGE (2.0 μg protein per lane). (**B**) 10% native PAGE (2.0 μg protein per lane). (**C**) Plot of thermal inactivation kinetics. E_0 and E_t are original activity and residual activity, respectively, after being heated for different time intervals. Data are the means of three experiments.

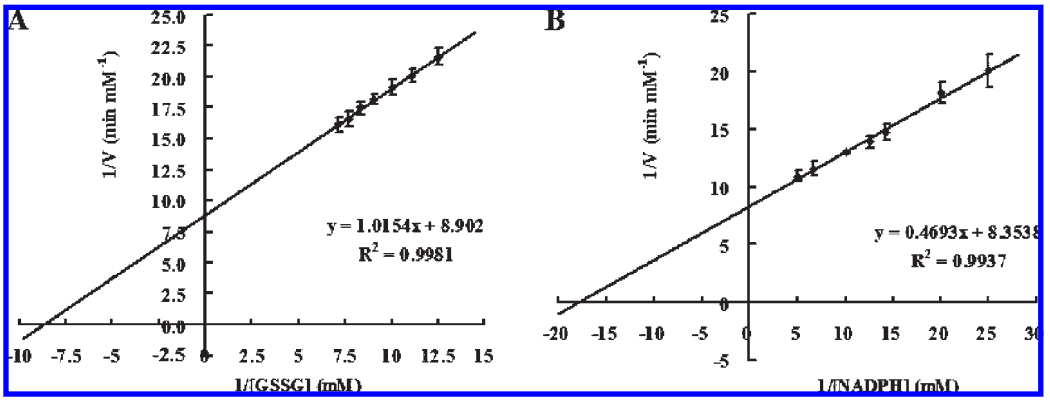

Figure 3. Double-reciprocal plot of varying GSSG and NADPH on IbGR activity. The initial rate of the enzymatic reaction was measured at 0.2 mM NADPH with the GSSG concentration varied from 0.08 to 0.14 mM (**A**). At 0.1 mM GSSG with the NADPH concentration varied from 0.04 to 0.2 mM (**B**). The K_m, V_{max}, and k_{cat} were calculated from Lineweaver−Burk plots.

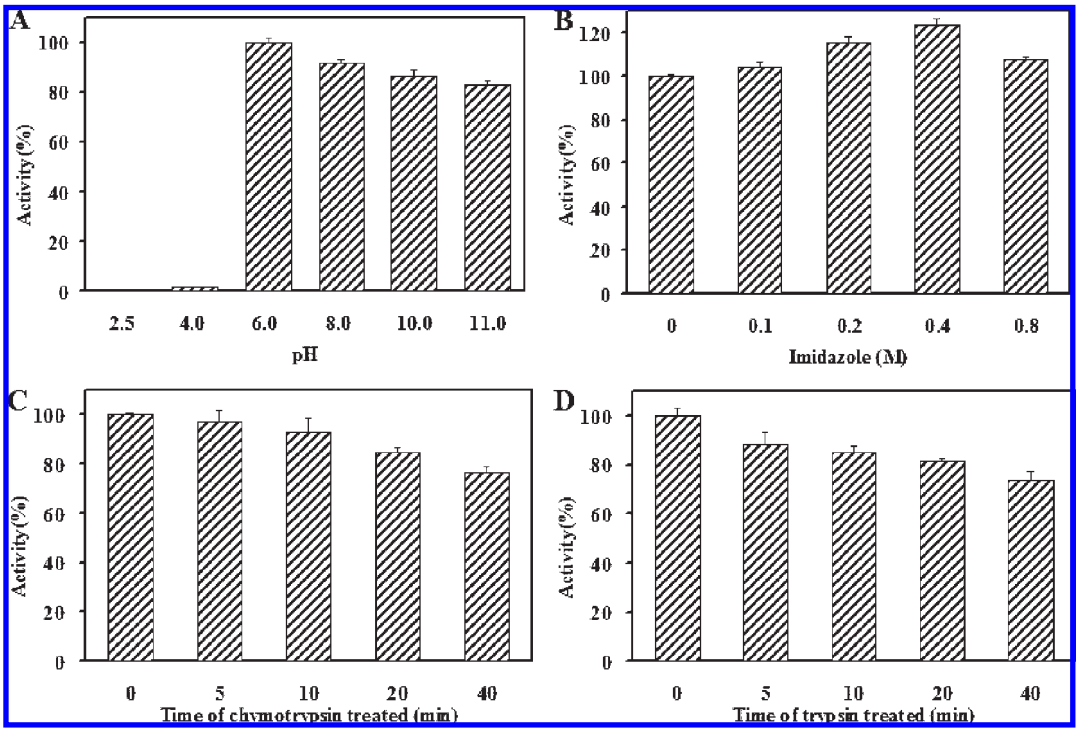

Figure 6. Effect of pH, imidazole, chymotrpsin, and trypsin on the purified IbGR. (**A**) The enzyme samples were incubated in buffers with different pH values at 37 °C for 1 h and then assayed for GR activity (0.2 μg protein/reaction). (**B**) The enzyme samples were incubated with various concentrations of imidazole at 37 °C for 1 h and then checked for activity (0.2 μg protein/reaction). (**C**) The enzyme samples were incubated with chymotrypsin at 37 °C for various times and then checked for GR activity (0.2 μg protein/reaction). (**D**) The enzyme samples were incubated with trypsin at 37 °C for various times and then checked for GR activity (0.2 μg protein/reaction). Data are the means of three experiments.

the first-order inactivation rate equation $\ln(E_t/E_0) = -K_d t$, where E_0 and E_t represent the original activity and the residual activity after heating for time t, respectively. The thermal inactivation rate constant (K_d) calculated for the enzyme at 70 °C was 3.48×10^{-1}, and the half-life of inactivation was 3.3 min (**Figure 5C**). IbGR has little or no activity at pH 4 or lower. However, the activity was stable in a broad pH range from 6.0 to 10.0 with an optimal pH of 6 (**Figure 6A**). Addition of imidazole up to 0.8 M has no significant effect on the activity (**Figure 6B**). The native enzyme was resistant to digestion by chymotrypsin or trypsin (**Figure 6C**,**D**) even at a high enzyme/substrate (w/w) ratio of 1/10. 1-Cys peroxiredoxin was used as a positive control in the protease digestion experiment. The peroxiredoxin was degraded within 20 min of treatment with either trypsin or chymotrypsin (results not shown).

DISCUSSION

This study reports the first cloning and expression of an important reduction enzyme, IbGR, from sweet potato. The biological active form of IbGR has been successfully expressed in yeast. We scanned the IbGR sequence against Swiss-Prot Prosite to locate potential post-translational modification sites. Although several potential phosphorylation sites (Ser193, Ser384, and Tyr365) were present, O-glycosylation sites (Ser488 and Thr492) were found. Further studies are required to determine if these post-translational modifications affect the structure and function of IbGR.

We compared the kinetic data of IbGR with that from other available sources. As shown in **Table 1**, Kaminaka et al. (*20*) reported that rice GR had K_m values of 92 μM and 39 μM for GSSG and NADPH, respectively. IbGR has higher K_m values for GSSG (114 μM) and NADPH (56 μM). A possible explanation for the discrepancy in the K_m values is that the sweet potato root is grown underground, whereas rice is exposed to air, ozone, UV light, among others causing higher oxidative stress. Therefore, it is reasonable to assume that rice would require more efficient GSSG to produce GSH for protection against oxidative stress.

Table 1. Kinetic Characterization of IbGR and Other Published GR[a]

		I. batatas	*O. sativa*	*E. coli*	bovine liver
GSSG	K_m (mM)	0.114	0.092	0.097	0.154
	k_{cat} (min^{-1})	3008.25			
	k_{cat}/K_m	26388.16			
NADPH	K_m (mM)	0.056	0.039	0.022	0.063
	k_{cat} (min^{-1})	3223.12			
	k_{cat}/K_m	57555.71			

[a] Values are from this work [*I. batatas* (*I. batatas* GR)] or from the literature (*O. sativa* (*O. sativa* GR (*20*)), *E. coli* (*E. coli* GR (*23*)), and bovine liver (bovine liver GR (*24*)).

Biochemists have always been interested in enzyme stabilities. The IbGR activity was strongly inhibited by Cu^{2+}, partially inhibited by Zn^{2+}, and unaffected by Ca^{2+}. It has been reported that *Saccharomyces cerevisiae* GR was inhibited by Cu^{2+} but not by Zn^{2+} (*21*). The enzyme is active at 70 °C with a half-life of 3.3 min at that temperature. It was evident that the recombinant IbGR was active in a broad pH range from 6 to 10 with optimal pH at 6.0. The activity was not affected by imidazole up to 0.8 M. It is possible that the imidazole ($pK_a = 6$) was keeping the enzyme close to its optimal pH.

The sweet potato IbGR protein contains potential trypsin cleavage sites and potential chymotrypsin-high specificity (C-term to [FYW], not before P) cleavage sites, or chymotrypsin-low specificity (C-term to [FYWML], not before P) cleavage sites. However, the native enzyme appeared to be resistant to digestion by trypsin or chymotrypsin even at a high enzyme/substrate (w/w) ratio of 1/10 (**Figure 6C**,**D**). The results suggested that IbGR may have a rigid structure and that the potential cleavage sites were

not accessible to the enzymes under the reaction conditions. It has been reported that proteins are attacked by trypsin less readily in their native state than when they are denatured (*22*).

In conclusion, we have cloned an IbGR cDNA and successfully expressed the enzyme in yeast. The recombinant enzyme showed high levels of activity and stability under various conditions. This information may be useful in formulating the enzyme as a possible antioxidant supplement.

LITERATURE CITED

(1) Lin, C. T.; Lin, M. T.; Chen, Y. T.; Shaw, J. F. Subunit interaction enhances enzyme activity and stability of sweet potato cytosolic Cu/Zn-superoxide dismutase purified by a His-tagged recombinant protein method. *Plant Mol. Biol*. **1995**, *28*, 303–311.

(2) Huang, D. J.; Chen, H. J.; Hou, W. C.; Lin, C. D.; Lin, Y. H. Active recombinant thioredoxin *h* protein with antioxidant activities from sweet potato (*Ipomoea batatas* [L.] Lam 'Tainong 57') storage roots. *J. Agric. Food Chem*. **2004**, *52*, 4720–4724.

(3) Huang, D. J.; Lin, C. D.; Chen, H. J.; Lin, Y. H. Antioxidant and antiproliferative activities of sweet potato (*Ipomoea batatas* [L.] Lam 'Tainong 57') constituents. *Bot. Bull. Acad. Sin*. **2004**, *52*, 179–186.

(4) Hou, W. C.; Chen, H. J.; Han, C. H.; Lin, C. Y.; Lin, Y. H. Glutathione peroxidase-like activity of 33 kDa trypsin inhibitor from roots of sweet potato (*Ipomoea batatas* (L.) Lam 'Tainong 57'). *Plant Sci*. **2004**, *166*, 1541–1546.

(5) Hou, W. C.; Han, C. H.; Chen, H. J.; Wen, C. L; Lin, Y. H. Storage proteins of two cultivars of sweet potato (*Ipomoea batatas* (L.) Lam) and their protease hydrolysates exhibited antioxidant activity in vitro. *Plant Sci*. **2005**, *168*, 449–456.

(6) Huang, G. J.; Chen, H. J.; Chang, Y. S.; Sheu, M. J.; Lin, Y. H. Recombinant sporamin and its synthesized peptides with antioxidant activities *in vitro*. *Bot. Stud*. **2007**, *48*, 133–140.

(7) Jiang, Y. C.; Huang, C. Y.; Wen, L.; Lin, C. T. Dehydroascorbate reductase cDNA from sweet potato (*Ipomoea batatas* [L.] Lam): expression, enzyme properties, and kinetic studies. *J. Agric. Food Chem*. **2008**, *56*, 3623–3627.

(8) Huang, G. J.; Sheu, M. J.; Chen, H. J.; Chang, Y. S.; Lin, Y. H. Growth inhibition and induction of apoptosis in NB4 promyelocytic leukemia cells by trypsin inhibitor from sweet potato storage roots. *J. Agric. Food Chem*. **2007**, *55*, 2548–2553.

(9) Noctor, G.; Foyer, C. Ascorbate and glutathione: keeping active oxygen under control. *Plant Mol. Biol*. **1998**, *49*, 249–279.

(10) Asada, K. The water−water cycle in chloroplast: scavenging of active oxygens and dissipation of excess photons. *Plant Mol. Biol*. **1999**, *49*, 601–639.

(11) Pastori, G.; Foyer, C. H.; Mullineaux, P. Low temperature induced changes in the distribution of H_2O_2 and antioxidants between the bundle sheath and mesophyll cells of maize leaves. *J. Exp. Bot*. **2000**, *51*, 107–113.

(12) Jimenez, A.; Hernandez, J. A.; de1 Rio, L. A.; Sevilla, F. Evidence for the presence of the ascorbate-glutathione cycle in mitochondria and peroxisomes of pea leaves. *Plant Physiol*. **1997**, *114*, 275–284.

(13) Rudhe, C.; Chew, O.; Whelan, J.; Glaser, E. A novel in vitro system for simultaneous import of precursor proteins into mitochondria and chloroplasts. *Plant J*. **2002**, *30*, 213–220.

(14) Chew, O.; Whelan, J.; Miller, A. H. Molecular definition of the ascorbate−glutathione cycle in *Arabidopsis* mitochondria reveals dual targeting of antioxidant defences in plants. *J. Biol. Chem*. **2003**, *278*, 46869–46877.

(15) Arnold, K.; Bordoli, L.; Kopp, J.; Schwede, T. The SWISS-MODEL workspace: A web-based environment for protein structure homology modelling. *Bioinformatics* **2006**, *22*, 195–201.

(16) Mittl, P. R. E.; Schulz, G. E. Structure of glutathione reductase from *Escherichia coli* at 1.86 Å resolution: Comparison with the enzyme from human erythrocytes. *Protein Sci*. **1994**, *3*, 799–809.

(17) Ken, C. F.; Hsiung, T. M.; Huang, Z. X; Juang, R. H.; Lin, C. T. Characterization of Fe/Mn-superoxide dismutase from diatom *Thallassiosira weissflogii*: cloning, expression, and property. *J. Agric. Food Chem*. **2005**, *53*, 1470–1474.

(18) Contour-Ansel, D.; Torres-Franklin, M. L.; Cruz, M. H.; d'Arcy-Lameta, A.; Zuily-Fodil, Y. Glutathione reductase in leaves of cowpea: cloning of two cDNAs, expression and enzymatic activity under progressive drought stress, desiccation and ABA treatment. *Ann. Bot*. **2006**, *98*, 1279–1287.

(19) Torres-Franklin, M. L.; Contour-Ansel, D.; Zuily-Fodil, Y.; Pham-Thi, A. Molecular cloning of glutathione reductase cDNAs and analysis of GR gene expression in cowpea and common bean leaves during recovery from moderate drought stress. *J. Plant Physiol*. **2008**, *165*, 514–521.

(20) Kaminaka, H.; Morita, S.; Nakajima, M.; Masumura, T.; Tanaka, K. Gene cloning and expression of cytosolic *glutathione* reductase in rice (*Oryza sativa* L.). *Plant Cell Physiol*. **1998**, *39*, 1269–1280.

(21) Serafini, M. T.; Romeu, A.; Arola, L. Zn(II), Cd(II) and Cu(II) interactions on glutathione reductase and glucose-6-phosphate dehydrogenase. *Biochem. Int*. **1989**, *18*, 793–802.

(22) Haurowitz, F.; Tunca, M.; Schwerin, P.; Göksu, V. The action of trypsin on native and denatured proteins. *J. Biol. Chem*. **1945**, *157*, 621–625.

(23) Bashir, A.; Perham, R. N.; Scrutton, N. S.; Berry, A. Altering kinetic mechanism and enzyme stability by mutagenesis of the dimer interface of glutathione reductase. *Biochem. J*. **1995**, *312*, 527–533.

(24) Ulusu, N. N.; Tandogan, B. Purification and kinetic properties of glutathione reductase from bovine liver. *Mol. Cell. Biochem*. **2007**, *303*, 45–51.

Received for Review January 5, 2009. Revised manuscript received March 17, 2009. Accepted March 27, 2009. This work was supported partially by the National Science Council of the Republic of China, Taiwan under Grant NSC 97-2313-B-019-001-MY3 to C.-T.L.